Haemodynamic responses to temperature changes of human skeletal muscle studied by laser-Doppler flowmetry

2012 Physiol. Meas. 33 1181

(http://iopscience.iop.org/0967-3334/33/7/1181)

IOP Publishing Physiological Measurement

Physiol. Meas. **33** (2012) 1181–1197 doi:10.1088/0967-3334/33/7/1181

Haemodynamic responses to temperature changes of human skeletal muscle studied by laser-Doppler flowmetry

Tiziano Binzoni[1,2], David Tchernin[2], Jonas Richiardi[2,3], Dimitri Van De Ville[2,3] and Jean-Noël Hyacinthe[2]

[1] Département de Neurosciences Fondamentales, University of Geneva, Geneva, Switzerland
[2] Département de l'Imagerie et des Sciences de l'Information Médicale, University Hospital, Geneva, Switzerland
[3] Institute of Bioengineering, Ecole Polytechnique Fédérale de Lausanne (EPFL), Lausanne, Switzerland

E-mail: tiziano.binzoni@unige.ch

Received 5 March 2012, accepted for publication 28 May 2012
Published 27 June 2012
Online at stacks.iop.org/PM/33/1181

Abstract

Using a small, but very instructive experiment, it is demonstrated that laser-Doppler flowmetry (LDF) at large interoptode spacing represents a unique tool for new investigations of thermoregulatory processes modulating the blood flow of small muscle masses in humans. It is shown on five healthy subjects that steady-state values of blood flow (perfusion) in the thenar eminence muscle group depend in a complex manner on both the local intramuscular temperature and local skin temperature, while the values of blood flow parameters measured during physiological transients, such as the post-ischaemic hyperhaemic response, depend only on the intramuscular temperature. In addition, it is shown that the so-called biological zero (i.e. remaining LDF signal during arterial occlusion) is influenced not only as expected by the intramuscular temperature, but also by the skin temperature. The proposed results reveal that the skeletal muscle has unique thermoregulatory characteristics compared, for example, to human skin. These and other observations represent new findings and we hope that they will serve as a stimulus for the creation of new experimental protocols leading to better understanding of blood flow regulation.

Keywords: blood flow regulation, biological zero, rest, ischaemia, cold, heat, local, temperature

(Some figures may appear in colour only in the online journal)

1. Introduction

The study of the influence of exogenous and/or endogenous temperature changes on blood flow regulation in the human skeletal muscle is one of the oldest domains of research in human physiology. After more than 70 years, this 'classical' domain is still very active because many fundamental questions have not yet been answered and old controversial issues are still debated (González-Alonso 2012).

Besides the difficulty of accounting for the multitude of physiological factors that, together with temperature, may influence the intramuscular blood flow—e.g., the size of the cooled/heated region (Heinonen *et al* 2011), intramuscular temperature gradients, muscle/skin temperature gradients (Webb 1995), hydration status (González-Alonso *et al* 1998), exercise intensity (Pearson *et al* 2011), mental stress (Blair *et al* 1959, Hamer *et al* 2006), hypnosis (Perry 1980), ageing (Kenney and Munce 2003) and specific pathologies (Johnson 1986, Mohan *et al* 1998)—the major problem remains the difficulty to measure blood flow (perfusion) itself (González-Alonso 2012).

Measurement techniques usually applied on humans, including venous occlusion plethysmography, ^{15}O PET, sestamibi ^{99m}Te SPECT, ^{133}Xe SPECT, first-pass iodinated contrast CT scan, first-pass Gd-chelates MRI, microbubble-assisted ultrasound, constant-infusion thermodilution technique and magnetic resonance imaging arterial spin labelling (Savard *et al* 1988, Bergmann *et al* 1984, Corbally and Brennan 1990, Feinstein 2004, Carlier *et al* 2006), have limitations that prevent them from being applied to some specific experimental protocols. For example, the necessity of investigating small regions of interest, or the non-invasiveness, or the need of a short sampling time during long and repeated periods, obviously represents a problem for some of the above techniques. It is important to note that temperature changes may also sometimes introduce artefacts in blood flow measurements (e.g., the temperature sensitivity of the MRI-based techniques; Binzoni *et al* 1995), rendering the technique inappropriate for studies on thermoregulation. Another constraint is that experimental protocols often work with water, because it is the most efficient way to cool/heat muscle masses. Techniques that are not compatible with this environment are not suitable in these cases.

For these reasons, the aim of this work was to continuously monitor non-invasively blood flow (perfusion) on small muscle masses at different temperatures. In his recent review, González-Alonso (2012) clearly highlights the fact that, due to methodological reasons, literature directly comparing heat and cold stress on haemodynamic responses to small human muscle masses is, unfortunately, sparse and that new technical solutions would thus be of extreme scientific interest. Actually, only one paper is cited as an example (Savard *et al* 1988), where the measurements were realized by venous occlusion plethysmography on the whole forearm. This was an important step, but the forearm always represents a relatively large muscle mass. Moreover, the forearm displays temperature gradients that are too large (Pennes 1948), and thus the measured blood flow cannot be reasonably related to a unique temperature.

This is why, in this contribution, we propose laser-Doppler flowmetry (LDF) at large interoptode spacing as a new and unique solution to study, non-invasively and in real time, localized intramuscular blood flow (perfusion) responses to temperature challenges. This approach will allow us to perform measurements on a very small muscle mass (e.g. hand muscles) with the investigated region of interest and the LDF detectors directly immersed in water environment (measurements in air represent a straightforward generalization). As an example, in the following sections it will be shown that LDF is able to detect the subtle differences existing in the dynamic and steady-state behaviour of the intramuscular blood flow (perfusion), for a given local temperature, when the temperature of a small skin surface

surrounding the muscle is varied. To our knowledge, the proposed results cannot be obtained with any other method. As a by-product of this work, we will present new physiological data that should serve as a further step in the understanding of the so-called biological zero (Tenland *et al* 1983), which corresponds to the LDF generated signal when the tissue blood flow (perfusion) is nil. We hope that this contribution will further boost this interesting domain by generating new ideas and experimental protocols infeasible in the past.

2. Material and methods

The aim of the present experimental protocol is (1) to heat/cool a small muscle mass to a given intramuscular temperature and (2) to show, using LDF, that intramuscular blood flow dynamics and the relative 'biological zero' can be influenced just by varying the skin temperature around this muscle. Dynamic blood flow changes, and the instauration of 'biological zero' levels, will be induced by the use of arterial occlusion. This protocol is used as an instructive example allowing us to explore the potential of LDF at large interoptode spacing for the study of exogenous and/or endogenous temperature changes on human skeletal muscle blood flow regulation. In the following text, we will use the expression 'blood flow' in the sense commonly accepted in LDF, i.e. the mean tissue 'blood perfusion' by capillaries, arterioles and venules. For this reason, we omit the reminder 'perfusion' in parenthesis as in the introduction.

2.1. Laser-Doppler flowmeter

A customized laser-Doppler flowmeter (Binzoni *et al* 2003, 2011), which allows working at large interoptode spacing (r), has been used. The laser-Doppler flowmeter consisted of a 785 nm laser source (IRLD50, Moor Instruments Ltd, UK) and a custom-made avalanche photo-detector (APD) module (Hamamatsu, Japan) with an active detection area of 1.5 mm diameter and a photo-electric sensitivity at 800 nm of 2.1×10^8 V W^{-1} (minimum detection limit 47 pW rms.). The cutoff frequency of the low-pass filter (anti-aliasing) of the APD module was 75 kHz (-3 dB). The cutoff frequency of the high-pass filter was 38 Hz. A 1.5 m multimode optical fibre (core diameter 400 μm), with a cylindric acetal probe head at the tissue/fibre interface, was connected to the laser. This gave a total of 45 mW of light at the probe head. A 1.5 m detection fibre (core 140 μm) was connected to the APD module with an identical probe head as that for the source fibre. All the probes were custom made (Moor Instruments Ltd, UK). The signal (voltage), representing the photo-electric current ($i(t)$) as a function of time (t), was directly acquired from the APD module output by using an analog-to-digital (ADC) acquisition card (NI USB-6251, National Instruments Corporation, Hungary). The ADC resolution was 16 bits and the input range was set to ± 5 V. The dc component of the measured laser-Doppler signals was always in the interval [0, 5] V. The ac modulation for the smallest signals was of the order of 10 mV, thus detectable by the ADC card. The sampling frequency was set to 1 MHz in order to cover all frequencies (ν) observed at the APD module output and to eliminate possible aliasing that may affect the desired LDF signals (Binzoni *et al* 2011). The number of sampled $i(t)$-points was $2^{17} = 131\,072$. The acquisition card was connected to a portable PC through a USB connection. The acquisition and data processing software was written in MATLAB® language (The Mathworks Inc., Natick, MA, USA).

Muscle mean blood speed (V), number of moving red blood cells ($\bar{n}$, often referred to inexactly as blood volume) and mean tissue blood flow ($\Phi = V\bar{n}$, often called perfusion) were then assessed in real time (in arbitrary units) from the zero- ($\langle\omega^{(0)}\rangle$) and first-order ($\langle\omega^{(1)}\rangle$) moment of the power density spectrum ($P(\omega)$) of $i(t)$ (Binzoni *et al* 2011):

$$\bar{n} \propto \langle\omega^{(0)}\rangle / i_0^2, \tag{1}$$

$$\Phi \propto \langle \omega^{(1)} \rangle / i_0^2, \tag{2}$$

$$V \propto \Phi / \bar{n}, \tag{3}$$

where

$$i_0 := \lim_{T \to +\infty} \frac{1}{2T} \int_{-T}^{T} i(t)\, \mathrm{d}t, \tag{4}$$

and

$$\left\langle \omega^{(n)} \right\rangle := \int_{-\infty}^{\infty} |\omega|^n P(\omega)\, \mathrm{d}\omega, \tag{5}$$

($n \in \{0, 1\}$), with

$$P(\omega) := \left| \int_{-\infty}^{\infty} i(t)\, \mathrm{e}^{-\mathrm{i}\omega t}\, \mathrm{d}t \right|^2, \tag{6}$$

and $\omega = 2\pi\nu$ the angular frequency.

The effect of the varying dc component on the noise level of the LDF instrument was also corrected as previously explained (Binzoni *et al* 2011).

2.2. Experimental protocol

Five healthy subjects, the authors, aged 38.2 ± 9.5 years, body mass 75.0 ± 6.3 kg, stature 181.6 ± 5.4 cm, participated in this non-invasive experiment. The subject, wearing light clothing to remain in the thermoneutral zone (Mekjavic *et al* 2003, Kingma *et al* 2012), was comfortably seated in a room at ∼24 °C, with the palmar aspect of the right arm laying on a rigid plastic support containing two non-invasive detectors: (1) a non-invasive intramuscular temperature probe (see section 2.3) and (2) the laser-Doppler optodes (r = 10 mm). These detectors were situated just under the thenar eminence (group of muscles on the palm of the human hand at the base of the thumb), and corresponding to the investigated region of interest. To prevent unwanted movements, the hand was secured to the plastic support by means of two Velcro straps. Watertightness was obtained by attaching the palm to the temperature probe with double-sided medical tape; the tape completely surrounded the optical probes. In this manner, the water could not reach the detectors and alter the measurements. Complementary to the Velcro straps, the double-sided tape appears to also be an effective means to prevent unwanted movements of the laser probe with respect to the hand. A standard pressure cuff was placed at the level of the right biceps.

The experiment started after having placed the probes and pressure cuff on the subject and after ∼20 min resting period at ambient temperature. This period of time was utilized to stabilize the intramuscular temperature probe and as such to reach a similar physiological condition for all subjects, and to optimize the LDF signals. Then, the subject's right arm and the relative support containing the probes were immersed in a thermostated bath with water temperature previously set at 15 °C, marking the beginning of the experiment. In this manner, the water was covering the hand and the forearm. The hand/forearm were lying horizontally at the bottom of the bath situated at the heart level. The water layer over the hand also has the advantage of strongly absorbing light, thus eliminating potential unwanted environmental light contamination. Continuous data acquisition of bath temperature (T_w), intramuscular temperature (T_m), $\bar{n}$ and Φ, immediately started after the arm immersion at a sampling time of 3.1 s. After 3 min baseline measurements, the pressure cuff was rapidly inflated to a supra-systolic pressure of 190 mmHg during 3 min to stop blood flow, and then rapidly deflated after

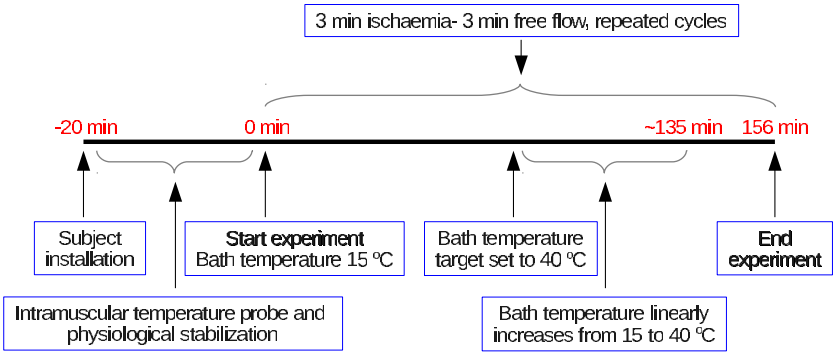

Figure 1. Time-line of the experimental protocol.

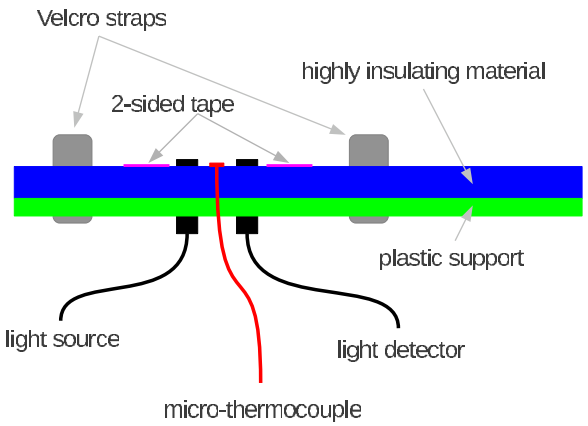

Figure 2. Schematic of the non-invasive intramuscular temperature probe. For explanatory purposes the proportions do not correspond to the real ones.

3 min. The inflation/deflation operation was repeated 26 times. The total measurement time was 156 min. After 93 min from the beginning of the experiment, the bath temperature was increased linearly from 15 to 40 °C and then stabilized at 40 °C (see figure 4(d), green line). The experimental protocol is summarized in figure 1. The thermostated system (heater HAAKE N6, cooler HAAKE C41, Karlsruhe, Germany) regulating the different water temperatures during the experiment was automatically controlled through a RS232c port by the same acquisition software and PC controlling the laser-Doppler.

2.3. Intramuscular and bath temperature measurements

Intramuscular temperature has been estimated non-invasively by using the insulated temperature probe method (Ranatunga *et al* 1987, Brajkovic *et al* 2006). A 14 mm layer of highly insulating material (Neoprene) was glued on the rigid plastic support where the right hand was fixed. A custom NT-type micro-thermocouple was fixed on its surface (see figure 2); copper and constantan wires, 28 and 10 μm diameter, respectively, inserted in a 0.2 mm (inner diameter) $\times$ 0.4 mm (outer diameter) sealed Teflon tube. The thermocouple was directly plugged into a NI USB-TC01 module connected to the PC through an USB port.

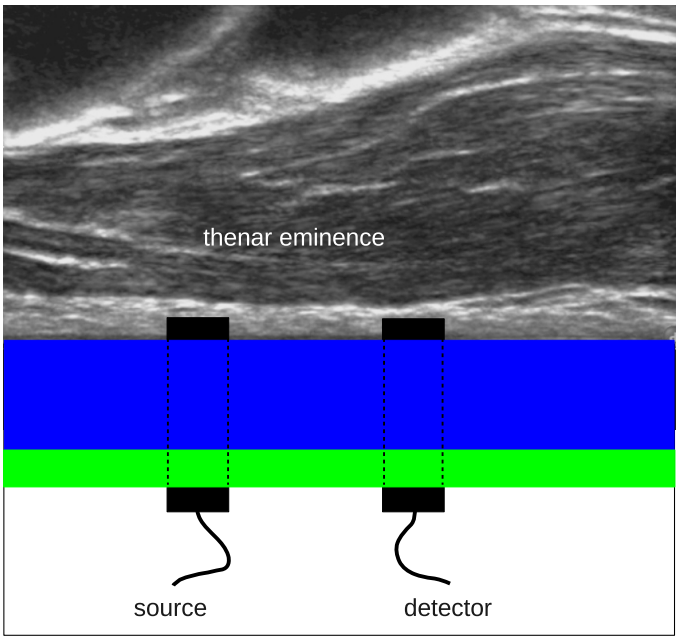

Figure 3. Thenar eminence of the right hand of one subject obtained by ultrasonography. The position of the optodes is represented on the image in a simplified view. For display purposes, the thicknesses of the highly insulating material and that of the rigid plastic support (see figure 2) are not to scale.

The micro-thermocouple was controlled, and the temperature was continuously recorded, by the same software controlling the laser-Doppler. The temperature probe needs to be installed on the subject 15–20 min before to the start of the measurements. After this period, the temperature of the thermocouple equals the intramuscular temperature a few mm under the skin.

A second thermocouple with its relative NI USB-TC01 module was used to record the temperature of the bath, always through the same software.

3. Results

3.1. Time dependence of $\bar{n}$, Φ, V, T_m and T_w

The parameters $\bar{n}$, Φ, V, T_m and T_w were measured on the thenar eminence of all subjects. The shape of the source and detector optodes was conceived in a way to minimize the potential remaining skin blood flow (in any case, negligible at this interoptode distance) by slightly pressing the skin surface. Figure 3 shows a schematic of the position of the optodes on an ultrasound image of one subject.

Figure 4 shows the behaviour of $\bar{n}$, Φ, V, T_m and T_w during the experimental protocol represented in figure 1. Before going through more quantitative results, let us make some observations by visual inspection of figure 4.

As expected, the effect of the ischaemia/reperfusion cycles on $\bar{n}$, Φ and V is nicely demonstrated by the presence of 'oscillations'.

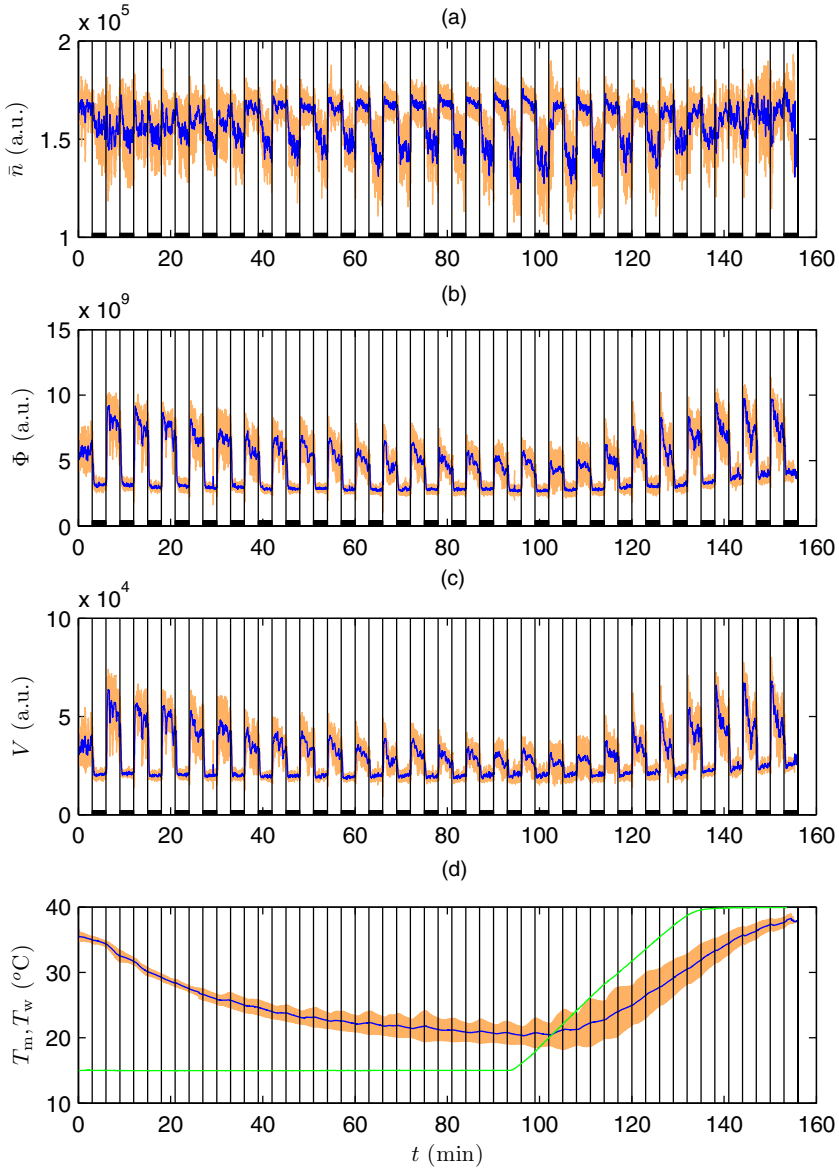

Figure 4. Data recorded on the human thenar muscles group during the experimental protocol appearing in figure 1 (mean of five subjects). Horizontal thick black bars, appearing on the abscissa, correspond to the ischaemic periods. $\bar{n}$: number of moving red blood cells; Φ: mean blood flow (perfusion); V: mean blood speed; T_m: intramuscular temperature; T_w: bath temperature (green line). a.u.: arbitrary units. The curves represent the mean of five subjects. The orange region represents the standard deviation. Standard deviation is not visible on T_w because it is too small.

During the ischaemic periods $\bar{n}$ (figure 4(a)) does not go to zero. The non-nil $\bar{n}$ level reached during ischaemia is classically called 'biological zero' (Tenland *et al* 1983) and, from the comparison of figures 4(a) and (d), it appears to depend on T_m, i.e. lower temperature lowers the 'biological zero'. This particular behaviour of $\bar{n}$ has the obvious consequence that Φ and V do not go to zero either during the ischaemic periods (figures 4(b) and (c)).

During the reperfusion intervals, Φ and V are related to T_m, i.e. Φ and V decrease with decreasing temperature (figures 4(b) and (c)), while a simple graphical inspection does not allow us to observe this phenomenon for $\bar{n}$ (figure 4(a)). After each ischaemic period, one can also observe the typical post-ischaemic hyperhaemic response, appearing as a Φ or V peak value. As expected, after the post-ischaemic peak, Φ or V decreases to a lower value. An hyperhaemic peak cannot be observed for $\bar{n}$.

It is interesting to note that the Φ and V levels during the first 3 min (where blood freely flows) are particularly low for the corresponding temperatures compared to the rest of the experiment. In fact, only after the first ischaemic period, the vascular system seems to reach a new physiological equilibrium that remains along the whole experiment.

To our knowledge, long lasting non-invasive intramuscular blood perfusion measurements, in real time and as a function of temperature, have never been performed before on humans. This is one of the interesting features of the LDF technique. In the following sections, we will better quantify the above qualitative observations made from figure 4. All statistical tests have been made at a significance level $\alpha = 0.01$.

3.2. Post-ischaemic intervals

3.2.1. Free blood flow. Figure 5 shows $\bar{n}$, Φ and V when the blood can flow freely (post-ischaemic periods) as a function of T_m. The $\bar{n}$, Φ, V and T_m values were taken as the mean over the last 31 s of the post-ischaemic periods appearing in figure 4 (i.e. means computed on the blue lines) and they are named $\bar{n}_{free}$, Φ_{free}, V_{free} and T_m, respectively (see also figure 6 for a graphical explanation).

Considering that in general the $\bar{n}$, Φ and V values may depend also on the temperature gradient existing between intramuscular and bath temperatures (see introduction), the data were divided into two groups: one group where $T_m \geqslant T_w$ and one where $T_m < T_w$.

To better quantify the behaviour of $\bar{n}_{free}$, Φ_{free} and V_{free} a linear model has been applied and the regression was significant for all the datasets appearing in figures 5(a), (b) and (c). The slopes of the couples of lines, for the conditions $T_m \geqslant T_w$ and $T_m < T_w$, are significantly different for $\bar{n}_{free}$, Φ_{free} and V_{free}.

The $\bar{n}_{free}$ versus T_m slope, for $T_m < T_w$, is significantly nil, while $\bar{n}_{free}$ is decreasing for increasing T_m for the group $T_m \geqslant T_w$. This means that after reperfusion the number of moving red blood cells returns to the same constant level at all the temperatures only if the intramuscular temperature is lower than the bath temperature. On the other hand, Φ_{free} and V_{free} are increasing for increasing T_m.

The blue markers at $T_m = 35.2\ ^\circ$C in figure 5 represent the free blood flow values for $\bar{n}$, Φ and V during the first 3 min of the experiment when the physiological system was not yet challenged by any ischaemic procedure (we will define them as: $\bar{n}_{35.2}$, $\Phi_{35.2}$ and $V_{35.2}$). Thus, the $\bar{n}_{35.2}$ value appearing in figure 5(a) is not significantly different from the $\bar{n}_{35.2}$ values of the $T_m < T_w$ group, while it is higher than the $T_m \geqslant T_w$ related data. The $\Phi_{35.2}$ (figure 5(b)) and $V_{35.2}$ (figure 5(c)) values are always lower than the theoretical corresponding Φ and V values for $T_m \geqslant T_w$ or $T_m < T_w$. Note that 3 min reperfusion is in principle enough to reach the starting baseline level because, before realizing the present protocol, preliminary tests (not shown) have been performed to ensure complete recovery. This is why this phenomenon is probably induced by physiological adaptations to temperature changes.

3.2.2. Post-ischaemic hyperhaemic response. The maximum values of $\bar{n}$, Φ and V attained just after reperfusion (during the first 31 s) at the different T_m (mean of five subjects) are reported in figure 7; they are denoted $\bar{n}_{max}$, Φ_{max} and V_{max}, respectively. As above the data have been divided into two groups: one group where $T_m \geqslant T_w$ and one where $T_m < T_w$.

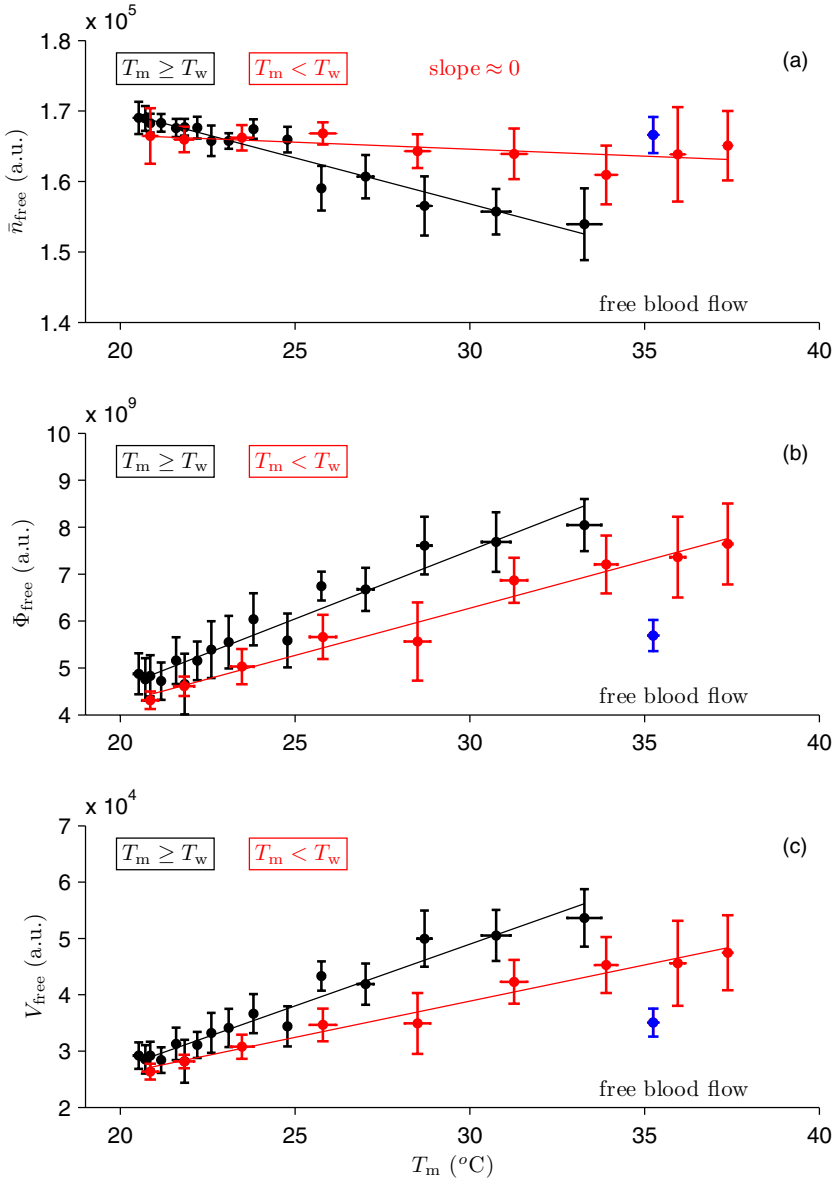

Figure 5. Data are derived from figure 4 (mean of five subjects). $\bar{n}_{free}$, Φ_{free} and V_{free} represent the mean intramuscular $\bar{n}$, Φ and V values, respectively, at different mean T_m obtained after 2.51 min reperfusion time. Black and red circles correspond to the condition $T_m \geqslant T_w$ and $T_m < T_w$, respectively. The blue circle at 35.2 °C is measured in a similar manner at the beginning of the experiment during the first 3 min (see figure 4). Lines are regression lines. The slope of the red line in panel (a) is significantly nil. The horizontal and vertical bars represent standard deviations.

To facilitate the discussion, the data have been represented with a linear model; however, contrary to the previous case appearing in figure 5, the lines were not statistically different when comparing the groups $T_m \geqslant T_w$ and $T_m < T_w$. This is why only one line appears on each figure panel. It is interesting to note that the slope of $\bar{n}_{max}$ versus T_m is significantly nil, and thus $\bar{n}_{max}$ always reaches the same peak level independently of the T_m or T_w values.

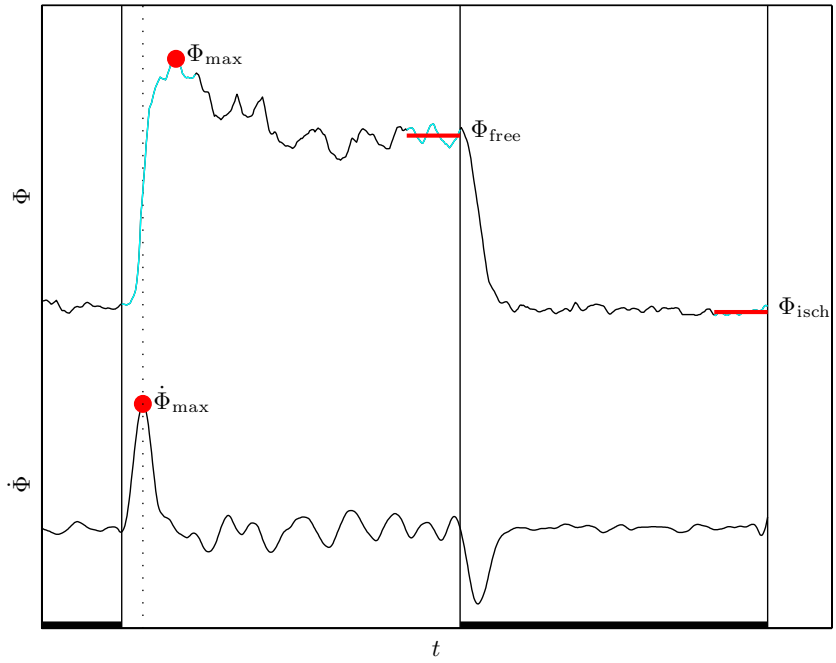

Figure 6. Schematic drawing explaining how the parameters $\dot{\Phi}_{max}$, Φ_{max}, Φ_{free} and Φ_{isch} are derived from figure 4. For the parameters $\dot{\bar{n}}_{max}$, $\bar{n}_{max}$, $\bar{n}_{free}$, $\bar{n}_{isch}$, $\dot{V}_{max}$, V_{max}, V_{free} and V_{isch} the procedure is analogous. $\dot{\Phi}_{max}$ is the time derivative of Φ_{max}. The horizontal black lines are ischaemic periods (arterial occlusion). The two horizontal red lines are the mean levels of the underlying cyan lines and represent the values for Φ_{free} and Φ_{isch} (static parameters). The red dots show the position where the values for $\dot{\Phi}_{max}$ and Φ_{max} are chosen (dynamic parameters).

3.2.3. Maximum $\bar{n}$, Φ and V time rates during reperfusion. Figure 8 reports the maximum values during reperfusion of the first-order time derivatives $\dot{\bar{n}}$, $\dot{\Phi}$ and $\dot{V}$ as a function of T_m (mean of five subjects), called $\dot{\bar{n}}_{max}$, $\dot{\Phi}_{max}$ and $\dot{V}_{max}$, respectively. The derivatives have been obtained by using the Savitzky–Golay algorithm (Savitzky and Golay, 1964). In this case as well, the data have been divided into two groups, one group where $T_m \geqslant T_w$ and one where $T_m < T_w$, but no statistical differences were detected between the two groups. Therefore, a single linear regression was applied to describe each variable. Figure 8(a) shows that $\dot{\bar{n}}_{max}$ decreases with increasing T_m. This means that at low temperatures the muscle has the tendency to recruit moving red blood cells at a higher speed in order to reach the target $\bar{n}_{max}$ (equal for all T_m), see figure 7(a). As opposed to $\dot{\bar{n}}_{max}$, figures 8(a) and (b) clearly show that $\dot{\Phi}_{max}$ and $\dot{V}_{max}$ increase as a function of T_m.

3.3. Ischaemic intervals

The data presented in figure 9 aim to investigate how the intramuscular 'biological zero' depends on temperature. The parameters $\bar{n}_{isch}$, Φ_{isch} and V_{isch} are mean values of $\bar{n}$, Φ and V (figure 4), respectively, computed over the last 31 s of the ischaemic intervals and are represented as a function of T_m (mean of five subjects). Figure 9(a) shows that $\bar{n}_{isch}$ increases with increasing T_m, but that the data groups defined by $T_m \geqslant T_w$ and $T_m < T_w$ are not significantly different. Therefore, only a simple linear regression is displayed. On the other

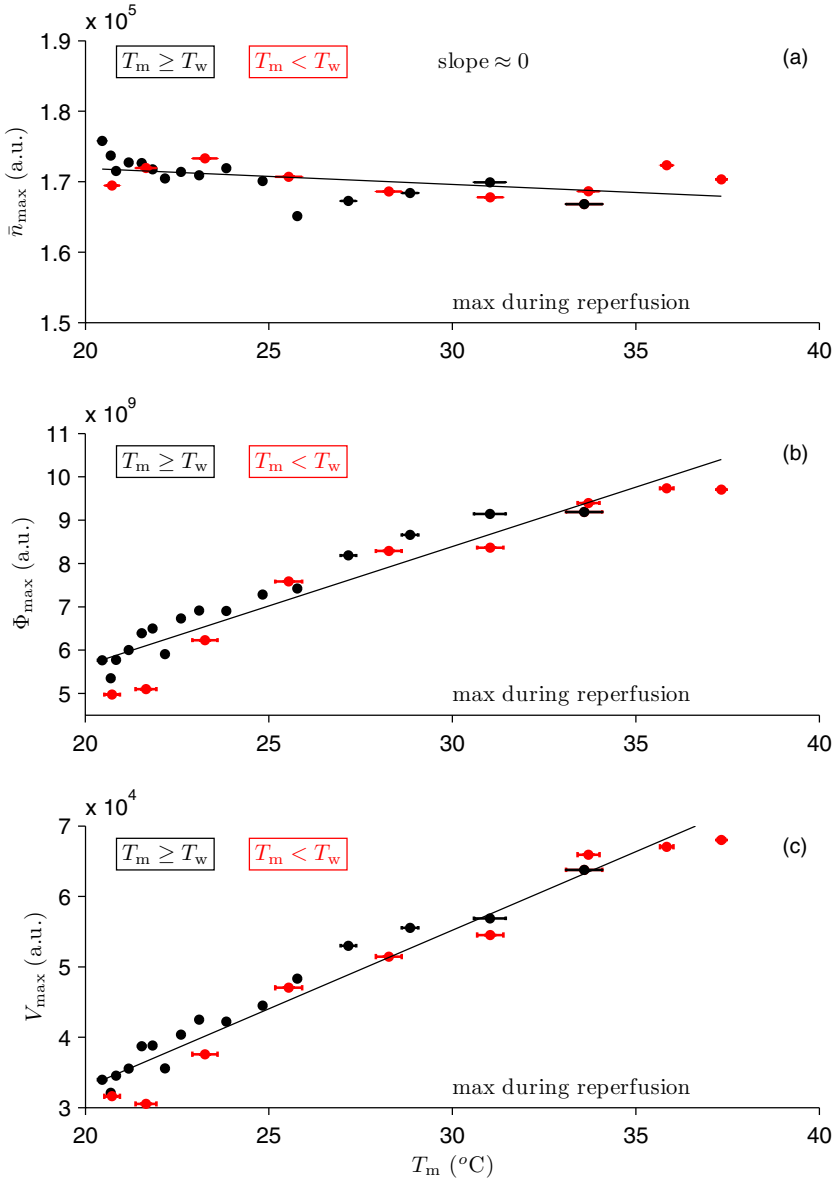

Figure 7. Data are derived from figure 4 (mean of five subjects). The circles represent the maximum values reached by $\bar{n}$, Φ and V during the reperfusion intervals as a function of T_m, denoted $\bar{n}_{max}$, Φ_{max} and V_{max}, respectively. Black and red circles represent the groups of data where $T_m \geqslant T_w$ and $T_m < T_w$, respectively. The black lines are the regression lines (of black and red points altogether). The slope in panel (a) is significantly nil. Horizontal bars represent standard deviations.

side, the physiological parameters Φ_{isch} and V_{isch} linearly increase for increasing temperature, with the exception of V_{isch} when $T_m \geqslant T_w$. In this case, the slope is significantly nil. In general, except for $\bar{n}_{isch}$, it appears that the behaviour of the groups defined by the constraints $T_m \geqslant T_w$ and $T_m < T_w$ is different. This is a new and extremely interesting observation

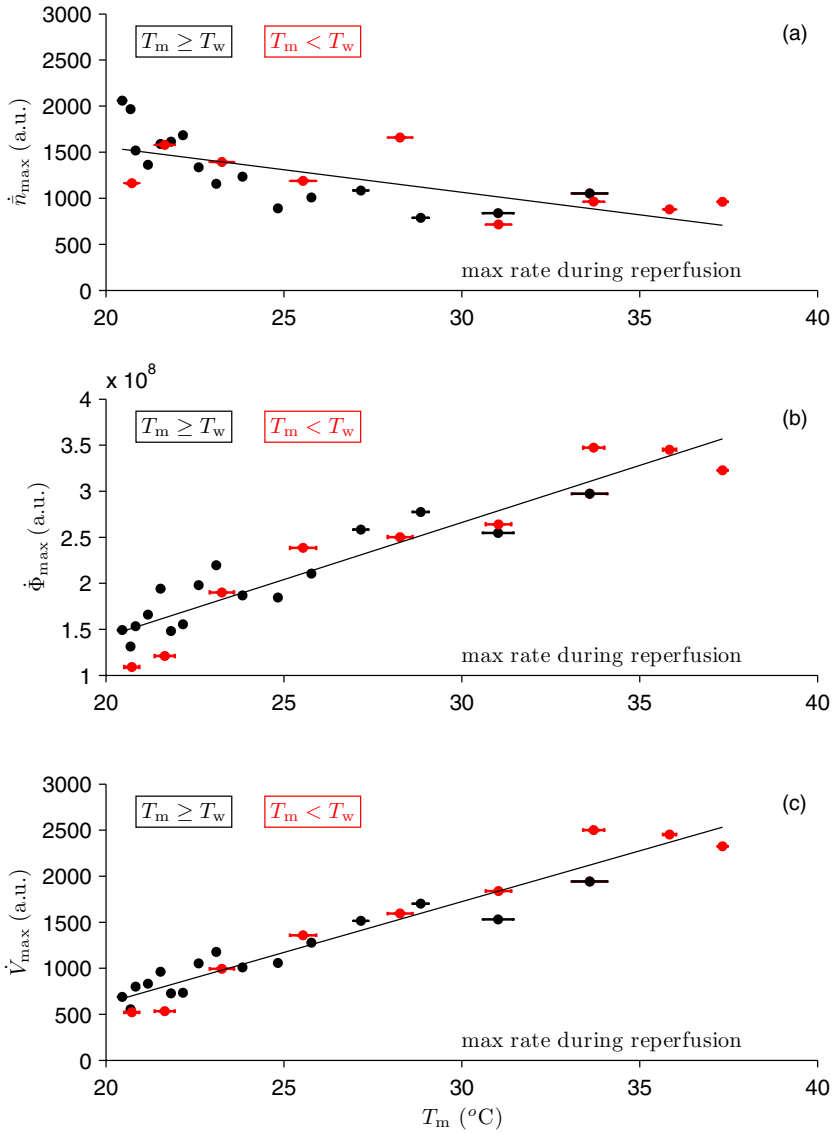

Figure 8. Data are derived from figure 4 (mean of five subjects). The circles represent the maximum speed of reperfusion (time derivative of $\bar{n}$, Φ and V) reached during the reperfusion intervals as a function of T_m, denoted $\dot{\bar{n}}_{max}$, $\dot{\Phi}_{max}$ and $\dot{V}_{max}$, respectively. Black and red circles represent the groups of data where $T_m \geqslant T_w$ and $T_m < T_w$, respectively. The black lines are the regression lines (of black and red points altogether). Horizontal bars represent standard deviations.

because it suggests that the T_m dependence of the 'biological zero' is dictated also by the neural modulation of the blood vessel and not only by a pure physical phenomenon (e.g., increase of Brownian motion of the moving particles for increasing T_m). This topic will be treated more specifically in the 'discussion and conclusions' section.

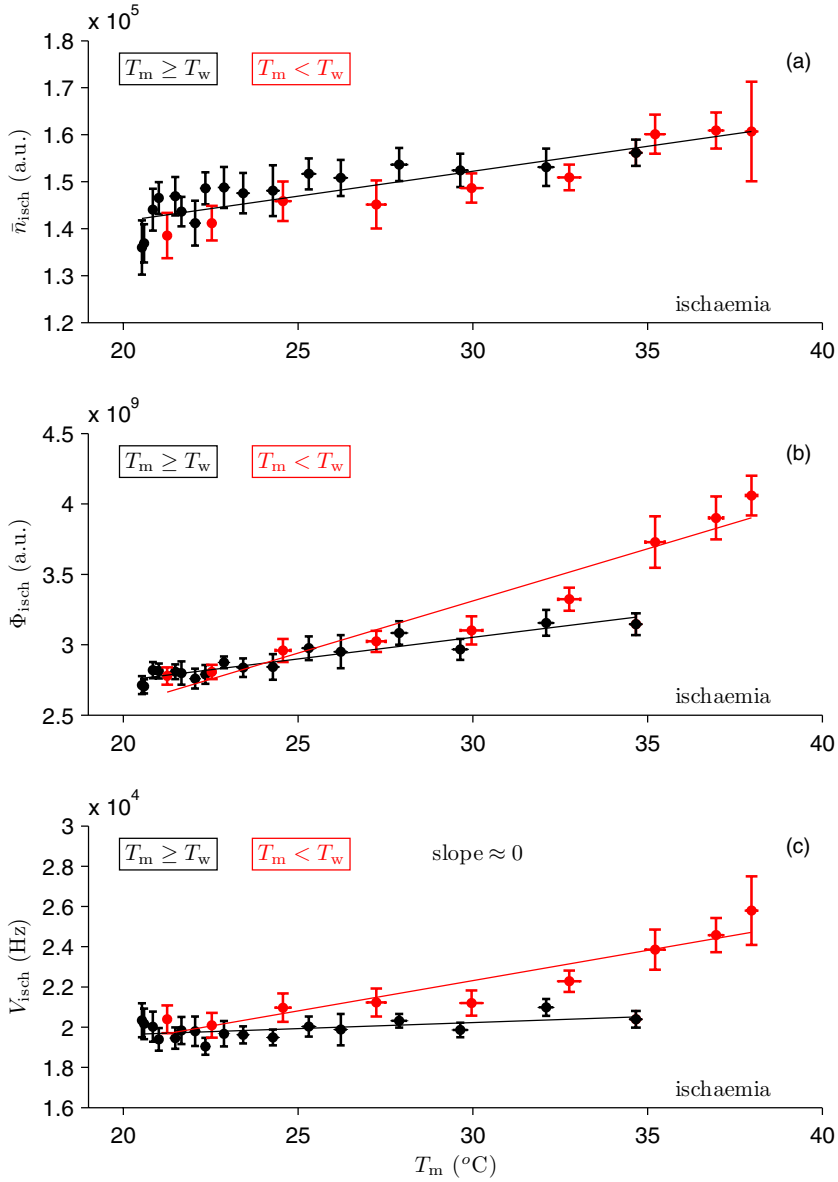

Figure 9. Data are derived from figure 4 (mean of five subjects). $\bar{n}_{\rm isch}$, $\Phi_{\rm isch}$ and $V_{\rm isch}$ represent the mean intramuscular $\bar{n}$, Φ and V values at different mean $T_{\rm m}$ obtained after 2.51 min of ischaemia, respectively. Black and red circles correspond to the condition $T_{\rm m} \geqslant T_{\rm w}$ and $T_{\rm m} < T_{\rm w}$, respectively. Lines are regression lines. The black regression line in panel (a) is for black and red points together (not significantly different). The horizontal and vertical bars represent standard deviations.

4. Discussion and conclusions

LDF at large interoptode spacing allows investigating the haemodynamics of the human muscolo-skeletal system (Binzoni *et al* 2003, 2011). Similar to the well-known near-infrared spectroscopy techniques, LDF light (photons) deeply penetrates in the tissue by following

a 'banana-shaped' path before to reach the detector fibre. For this reason, in the present experiment on human thenar eminence, one can reasonably consider that blood-flow-related information contained in the LDF signal mainly originates from the muscle. In fact, the LDF signal is essentially explained by the total phase change of each single photon during its travel from the source fibre tip to the detector fibre tip. Specifically, the total phase change of a photon is the accumulation of single phase changes due to interactions with red blood cells. The majority of the interactions occur in the muscle, because the contribution from the extremities of the path, e.g. the piece of path inside the skin just under the fibre tips, is negligible (fraction of mm) compared to the rest of the path in the muscle (many cm). For this reason, we can consider as a good approximation that the phase contribution of all the photons to the LDF signal, and thus to the flow information, comes from the muscle. In addition, since the skeletal muscle (red tissue) has a very high capillary concentration compared, e.g., to the fat tissue (white tissue), this definitively increases the probability of having scattering events with red blood cells and thus the weight of muscle blood flow in the LDF signal.

For the first time, we have applied LDF to the specific study of thermoregulatory processes in the skeletal muscle. The first goal has been attained by monitoring non-invasively and in real time, $\bar{n}$, Φ and V as a function of T_m and T_w. Data were collected continuously during 156 min without any discomfort for the subject. These data reveal that dynamic parameters, such as $\bar{n}_{max}$, Φ_{max} and V_{max} (figure 7) or $\dot{\bar{n}}_{max}$, $\dot{\Phi}_{max}$ and $\dot{V}_{max}$ (figure 8), behave in a different manner as a function of T_m and T_w compared to static ones such as $\bar{n}_{free}$, Φ_{free} and V_{free} (figure 5) or $\bar{n}_{isch}$, Φ_{isch} and V_{isch} (figure 9). In fact, dynamic parameters appear to be T_w-independent and they change their value only as a function of T_m. This is reflected here by the fact that dynamic values do not depend on $T_m \geqslant T_w$ and $T_m < T_w$. Thus, for the given experimental conditions, fast haemodynamic adaptations do not depend on the sign of the skin–muscle temperature gradient, but steady levels, such as Φ_{free}, do (the only exception being $\bar{n}_{isch}$). To our knowledge, this observation has never been made before in human subjects. The reason for this particular behaviour remains to be explained and certainly opens the way to new research topics.

Figure 5 conveys more information on how Φ_{free} is regulated as a function of T_m and T_w. Panel (a) (red circles) shows that if $T_m < T_w$, then $\bar{n}_{free}$ remains constant and independent of T_m. This means that in this case the observed increase/decrease in Φ_{free} (panel b) is not determined by a vasodilation/vasoconstriction but by an increase/decrease in V_{free}. Changes in V_{free} may be explained by the usual modulation of the diameter of the pre-capillary sphincters (intuitively, if we open/close a water tap, we can change the flow without changing the diameter/volume of the tubes). On the other hand, if $T_m \geqslant T_w$, then $\bar{n}_{free}$ (panel a, black circles) is no longer a constant, but appears to decrease with increasing T_m. In this case, the T_m dependence of Φ_{free} is determined by a simultaneous and opposite change in $\bar{n}_{free}$ and V_{free}. When $T_m \geqslant T_w$, then the muscle vessels may remain more 'vasoconstricted' at high T_m, but the combined effect of the opposite change in $\bar{n}_{free}$ and V_{free} is a larger Φ_{free} value than for the $T_m < T_w$ condition. Considering that at rest a local increase in T_m induces in humans a series of physical and metabolic changes (Binzoni *et al* 2000) which imply an increase in oxygen consumption (Binzoni *et al* 2002), Φ_{free} must in any case adapt to the new oxygen needs, and this is compatible with our observations. Note that Φ_{free} values are globally higher for $T_m \geqslant T_w$ compared to $T_m < T_w$. This Φ_{free}-overcompensation is probably induced by the combined necessity of temperature regulation and oxygen transport, but the exact reason remains to be explained and will certainly be matter for future work.

'Biological zero' has been largely studied, experimentally and theoretically, in human skin (Tenland *et al* 1983, Caspary *et al* 1988, Wahlberg *et al* 1992, Abbot and Beck 1993, Colantuoni *et al* 1993, Zhong *et al* 1998, Kernick *et al* 1999); however, its behaviour as a

function of temperature has never been shown for the human skeletal muscle. Moreover, it is not yet clear if a local/central nervous drive influencing vasomotion may contribute to the 'biological zero' modulation. In this contribution, the experimental protocol has been built in a way to potentially generate different 'vascular drives' (Webb 1995) for the same local T_m, and this by changing T_w locally. In figure 9, we appreciate the influence of this physiological manipulation on the 'biological zero' for the three related parameters $\bar{n}_{isch}$, Φ_{isch} and V_{isch}. The observed differences between the two groups $T_m \geqslant T_w$ and $T_m < T_w$ (panels b and c) cannot be explained by a simple physical effect due to temperature, because for same T_m we have two different (red and black) values, for Φ_{isch} and V_{isch}, respectively. A physical effect would generate the same values for each parameter. Interestingly, this phenomenon is not observed for $\bar{n}_{isch}$, where only a global increase as a function of T_m is measured. Thus, when the ambient temperature is lower than the muscle temperature, the 'vascular component' V_{isch} seems to be maintained to a unique value (panel c, black) while the number of moving particles (produced by the vascular movement) slightly increases (panel a, black). A global increase of Φ_{isch} as a function of T_m has already been observed for the skin (Kernick *et al* 1999), but the difference between the groups based on $T_m \geqslant T_w$ versus $T_m < T_w$ is a new finding. Even in this case, the physiological mechanism underlying this phenomenon needs to be better understood.

For the sake of completeness, we would like to note that the high-pass filter (38 Hz) included in the instrument might theoretically 'hide' a fraction of the signal during ischaemia, and thus introducing a potential artefact in the measurements. In fact, during ischaemia red blood cells drastically slow down their velocity (Brownian-like movement) and the phase shift accumulated by the photons decreases in magnitude. This is equivalent to observing smaller frequency shifts that might 'disappear' from the LDF signal if <38 Hz. However, it must be noted that LDF at large optode spacing is less sensitive to this phenomenon compared to classical short distance LDF (fraction of mm). This is because even a very slow movement in red blood cells induces a relatively large phase change (i.e. a large frequency shift) due to the higher number of interactions with moving scatterers occurring along the long photon travelling path. This 'pushes' the frequencies out of the high-pass filter. Moreover, an LDF variable such as Φ is in practice not sensitive to this phenomenon because it is derived by means of the first-order moment (5) where the ponderation factor ω has, by definition, very small values in the filter range. This further decreases the possibility of the filter artefact. Finally, it is important to note that, even in the worst case, the commonly observed difference between the $T_m \geqslant T_w$ and $T_m < T_w$ groups, for a given T_m, is not an effect of the high-pass filter, but is purely physiological. In fact, for the same T_m, the high-pass filter can obviously not arbitrarily split the data into two groups.

Last but not least, the dynamic parameters appear not to depend on T_w but only on T_m (figures 7 and 8). The increase of post-ischaemic Φ_{max} for increasing T_m (figure 7(b)) is determined only by the change in the mean blood speed (pre-capillary sphincters modulation) and not by a vasodilation, because $\bar{n}_{max}$ always attains the same constant value (panel a). From figure 8, it also appears that the maximum rate of change of the dynamic parameters is independent of T_w, and thus the vascular system tries to adapt with a maximum rate that depends only on T_m. However, in this case $\dot{\bar{n}}_{max}$ decreases with increasing T_m. This means that the system has the tendency to take more time to reach the maximum constant $\bar{n}_{max}$ level at high temperatures. In general, dynamic parameters display a coarser regulation because they depend only on T_m and not on the exogenous temperature at the skin level. The reason of this behaviour merits further investigation.

From the technical point of view, the power of the laser light source used in the present instructive experiment is higher that the values utilized, e.g., in a clinical environment. This

problem can be solved by using a weaker laser and many detectors in parallel, or by increasing the surface of the source fibre tip with a light diffuser.

In conclusion, this small but instructive experiment has demonstrated that LDF at large interoptode spacing is a unique tool allowing new investigations on thermoregulatory processes modulating the blood flow of small muscle masses in humans. We hope that this example will lead to novel and original protocols in this domain.

Acknowledgments

The authors kindly thank Dr Ronald Hogg for personal sponsoring of the special photo-detector for the LDF instrumentation. This work has been supported in part (JR, JNH) by the Center for Biomedical Imaging (CIBM).

References

Abbot N C and Beck J S 1993 Biological zero in laser Doppler measurements in normal, ischaemic and inflamed human skin *Int. J. Microcirc. Clin. Exp.* **12** 89–98

Bergmann S R, Fox K A, Rand A L, McElvany K D, Welch M J, Markham J and Sobel B E 1984 Quantification of regional myocardial blood flow *in vivo* with $H_2{}^{15}O$ *Circulation* **70** 724–33

Binzoni T, Boggett D and Van De Ville D 2011 Laser-Doppler flowmetry at large interoptode spacing in human tibia diaphysis: Monte Carlo simulations and preliminary experimental results *Physiol. Meas.* **32** N33–53

Binzoni T, Hiltbrand E, Kayser B, Ferretti G and Terrier F 1995 Human intramuscular temperature and heat flow transients at rest *J. Appl. Physiol.* **79** 1736–43

Binzoni T, Hiltbrand E, Terrier F, Cerretelli P and Delpy D 2000 Temperature dependence of human gastrocnemius pH and high-energy phosphate concentration by noninvasive techniques *Magn. Reson. Med.* **43** 611–4

Binzoni T, Leung T S, Boggett D and Delpy D 2003 Non-invasive laser Doppler perfusion measurements of large tissue volumes and human skeletal muscle blood RMS velocity *Phys. Med. Biol.* **48** 2527–49

Binzoni T, Ngo L, Hiltbrand E, Springett R and Delpy D 2002 Non-standard O(2) consumption-temperature curves during rest and isometric exercise in human skeletal muscle *Comp. Biochem. Physiol. A: Mol. Integr. Physiol.* **132** 27–32

Blair D A, Glover D E, Greenfield A D and Roddie I C 1959 Excitation of cholinergic vasodilator nerves to human skeletal muscles during emotional stress *J. Physiol.* **148** 633–47

Brajkovic D, Ducharme M B, Webb P, Reardon F D and Kenny G P 2006 Insulation disks on the skin to estimate muscle temperature *Eur. J. Appl. Physiol.* **97** 761–5

Carlier P G, Bertoldi D, Baligand C, Wary C and Fromes Y 2006 Muscle blood flow and oxygenation measured by NMR imaging and spectroscopy *NMR Biomed.* **19** 954–67

Caspary L, Creutzig A and Alexander K 1988 Biological zero in laser Doppler fluxmetry *Int. J. Microcirc. Clin. Exp.* **7** 367–71

Colantuoni A, Bertuglia S and Intaglietta M 1993 Biological zero of laser Doppler fluxmetry: microcirculatory correlates in the hamster cheek pouch during flow and no flow conditions *Int. J. Microcirc. Clin. Exp.* **13** 125–36

Corbally M T and Brennan M F 1990 Noninvasive measurement of regional blood flow in man *Am. J. Surg.* **160** 313–21

Feinstein S B 2004 The powerful microbubble: from bench to bedside, from intravascular indicator to therapeutic delivery system, and beyond *Am. J. Physiol. Heart Circ. Physiol.* **287** H450–7

González-Alonso J 2012 Human thermoregulation and the cardiovascular system *Exp. Physiol.* **97** 340–6

González-Alonso J, Calbet J A and Nielsen B 1998 Muscle blood flow is reduced with dehydration during prolonged exercise in humans *J. Physiol.* **513** 895–905

Hamer M, Boutcher Y N, Park Y and Boutcher S H 2006 Reproducibility of skeletal muscle vasodilatation responses to Stroop mental challenge over repeated sessions *Biol. Psychol.* **73** 186–9

Heinonen I, Brothers R M, Kemppainen J, Knuuti J, Kalliokoski K K and Crandall C G 2011 Local heating, but not indirect whole body heating, increases human skeletal muscle blood flow *J. Appl. Physiol.* **111** 818–24

Johnson J M 1986 Nonthermoregulatory control of human skin blood flow *J. Appl. Physiol.* **61** 1613–22

Kenney W L and Munce T A 2003 Invited review: aging and human temperature regulation *J. Appl. Physiol.* **95** 2598–603

Kernick D P, Tooke J E and Shore A C 1999 The biological zero signal in laser Doppler fluximetry—origins and practical implications *Pflugers Arch.* **437** 624–31

Kingma B, Frijns A and van Marken Lichtenbelt W 2012 The thermoneutral zone: implications for metabolic studies *Front. Biosci.* **4** 1975–85

Mekjavic I B, Tipton M J and Eiken O 2003 Thermal considerations in diving *Bennett and Eliott's Physiology and Medicine of Diving* 5th edn, ed A O Brubakk and T S Neuman (London: Saunders)

Mohan J, Marshall J M, Reid H L, Thomas P W, Hambleton I and Serjeant G R 1998 Peripheral vascular response to mild indirect cooling in patients with homozygous sickle cell (SS) disease and the frequency of painful crisis *Clin. Sci.* **94** 111–20

Pearson J, Low D A, Stöhr E, Kalsi K, Ali L, Barker H and González-Alonso J 2011 Hemodynamic responses to heat stress in the resting and exercising human leg: insight into the effect of temperature on skeletal muscle blood flow *Am. J. Physiol. Regul. Integr. Comp. Physiol.* **300** R663–73

Pennes H H 1948 Analysis of tissue and arterial blood temperatures in the resting human forearm *J. Appl. Physiol.* **1** 93–122

Perry B J 1980 Control of physiological phenomena via hypnosis with special reference to contraception *Aust. J. Clin. Hypnother.* **1** 73–7

Ranatunga K W, Sharpe B and Turnbull B 1987 Contractions of a human skeletal muscle at different temperatures *J. Physiol.* **390** 383–95

Savard G K, Nielsen B, Laszczynska J, Larsen B E and Saltin B 1988 Muscle blood flow is not reduced in humans during moderate exercise and heat stress *J. Appl. Physiol.* **64** 649–57

Savitzky A and Golay M J E 1964 Smoothing and differentiation of data by simplified least squares procedures *Anal. Chem.* **36** 1627–39

Tenland T, Salerud E G, Nilsson G E and Oberg P A 1983 Spatial and temporal variations in human skin blood flow *Int. J. Microcirc. Clin. Exp.* **2** 81–90

Wahlberg E, Olofsson P, Swedenborg J and Fagrell B 1992 Effects of local hyperemia and edema on the biological zero in laser Doppler fluxmetry (LD) *Int. J. Microcirc. Clin. Exp.* **11** 157–65

Webb P 1995 The physiology of heat regulation *Am. J. Physiol.* **268** R838–50

Zhong J, Seifalian A M, Salerud G E and Nilsson G E 1988 A mathematical analysis on the biological zero problem in laser Doppler flowmetry *IEEE Trans. Biomed. Eng.* **45** 354–64